Li, F. et al. Evidence for an internal entropy contribution to phosphoryl transfer: a study of domain closure, backbone flexibility, and the catalytic cycle of cAMP-dependent prote...

ARTICLE *in* JOURNAL OF MOLECULAR BIOLOGY · FEBRUARY 2002

Impact Factor: 4.33 · DOI: 10.1006/jmbi.2001.5256 · Source: PubMed

6 AUTHORS, INCLUDING:

Celina E Juliano
University of California, Davis
21 PUBLICATIONS **1,253** CITATIONS

SEE PROFILE

doi:10.1006/jmbi.2001.5256 available online at http://www.idealibrary.com on IDEAL® J. Mol. Biol. (2002) 315, 459–469

JMB

Evidence for an Internal Entropy Contribution to Phosphoryl Transfer: A Study of Domain Closure, Backbone Flexibility, and the Catalytic Cycle of cAMP-Dependent Protein Kinase

Fei Li[1], Milind Gangal[1], Celina Juliano[2], Elliot Gorfain[2], Susan S. Taylor[2] and David A. Johnson[1]*

[1]*Division of Biomedical Sciences, University of California, Riverside CA 92521-0121, USA*

[2]*Howard Hughes Medical Institute, Department of Chemistry and Biochemistry School of Medicine, University of California, San Diego, La Jolla, CA 92093-0359, USA*

**Corresponding author*

While there is no question that ligands can induce large-scale domain movements that narrow (close) the active-site cleft of the catalytic (C) subunit of cAMP-dependent protein kinase (cAPK), the results from small-angle X-ray scattering, protein footprinting, and thermostability studies are inconsistent with regard to which ligands induce these movements. This inconsistency suggests a greater complexity of cAPK conformational dynamics than is generally recognized. As an initial step to study this issue in relation to the catalysis, a new method to measure cAPK domain closure was developed, and the state of domain closure and the local segmental flexibility at major steps of the cAPK catalytic cycle were examined with site-directed labeling and fluorescence spectroscopy. To achieve this, a C subunit mutant (F239C/C199A) was engineered that allowed for fluorescein 5-maleimide (donor) conjugation of F239C in the large lobe and tetramethylrhodamine (acceptor) conjugation of C343 in the small lobe. Domain closure was assessed as an increase in the efficiency of energy transfer between donor and acceptor. The anisotropy decay of fluoroscein 5-maleimide, conjugated to a site of cysteine substitution (K81C) in the small lobe of the C subunit was used to assess the local backbone flexibility around the B helix. The effects of substrate/pseudosubstrate (ATP and PKI(5-24)), a fragment of protein kinase inhibitor) and products (ADP and phosphorylated PKS) on domain closure and B helix flexibility were measured. The results show that domain closure is not tightly coupled to the flexibility around K81C. Moreover, although substrates/pseudosubstrate and products independently close the active-site cleft, only the substrates substantially decreased the backbone flexibility around the B helix. Because this order-to-disorder transition coincides with the phosphoryl transfer transition, the results suggest the existence of an internal entropy contribution to catalysis.

Keywords: cAMP-dependent protein kinase; fluorescent resonance energy transfer; time-resolved fluorescence anisotropy; entropy; conformational flexibility

Present address: M. Gangal, Beth Israel Deaconess Medical Center, 99 Brookline Avenue, RN/548, Boston, MA 02215, USA.

Abbreviations used: cAMP, adenosine 3′,3′-phosphate; cAPK, cAMP-dependent protein kinase; C subunit, the α isoform of the catalytic subunit of cAPK; D/A, dipolar energy transfer donor and acceptor; f_{xb}, fraction of the observed anisotropy decay associated with the ''fast'' depolarization processes; ϕ_{fast}, fast rotational correlation time; ϕ_{slow}, slow rotational correlation time; FRET, fluorescence resonance energy transfer; FM, fluorescein-5-maleimide; TMRM, tetramethylrhodamine-5-maleimide; PKI(5-24), a fragment (residues 5-24) of the α isoform of the heat-stable protein kinase inhibitor (TTYADFIASGRTGRRNAIHD, numbering based on full-length PKI(1-75)); PKI(5-22)amide, a fragment (residues 5-22) of the α isoform of the heat-stable protein kinase inhibitor (TTYADFIASGRTGRRNAI-NH_2; PO_4-PKS, phosphorylated adduct of TTYADFIASGRTGRRASIHD; TRFA, time-resolved fluorescence anisotropy.

E-mail address of the corresponding author: david.johnson@ucr.edu

0022-2836/02/030459–11 $35.00/0

Introduction

Kinases catalyze the transfer of the γ-phosphate group from ATP (occasionally from other nucleoside triphosphates) to hydroxyl acceptors. Substrate binding to kinases has long been recognized to induce large-scale conformational changes that involve the narrowing (closing) of the active-site cleft formed by two adjacent lobes. Although the structure of these two lobes is conserved among all kinases, the orientation of the nucleotide and the site of phosphoryl transfer differ. The first crystallographic evidence for this ligand-induced domain closure phenomenon stems from the study of hexokinase, where the apo (open) and glucose-bound (closed) configurations were compared.[1] More recently, small-angle X-ray scattering results and the X-ray crystallographic analysis of the catalytic (C) subunit of cAMP-dependent protein kinase (cAPK) in different liganded states reveal the existence of a related domain movement or closure.[2–8] For the cAPK C subunit, domain closure involves both a hinge and sliding motion of the smaller lobe toward the larger lobe. The superposition of the so-called open and closed conformations of the C subunit shows that most of this movement is confined to the small lobe (Figure 1(a)). The function of large-scale domain movement appears to be essential for the proper positioning of the reactants for specific phosphoryl transfer to hydroxyl groups in target substrates.

While there is little doubt that the cAPK C subunit undergoes ligand-induced domain closure, conflicting evidence exists as to which ligands

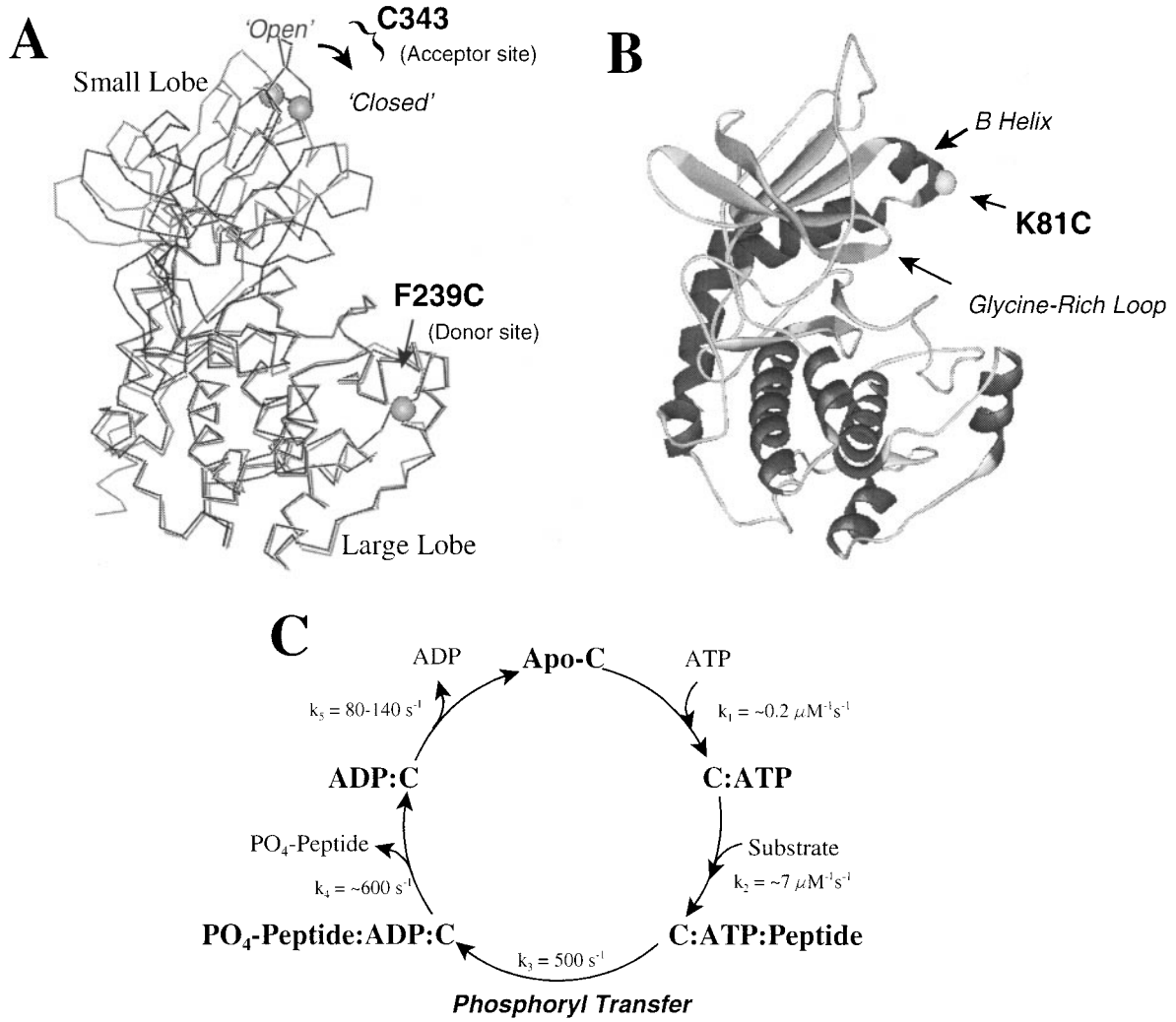

Figure 1. Superimposition of open and closed conformations of the C subunit and cAPK catalytic cycle. (a) Superimposition of the PKI(5-24):C binary open complex (faint lines; PDB code 1ctp) and the ATP:PKI(5-24):C ternary closed complex (dark lines; PDB code 1atp) with ATP and PKI(5-24) not shown. The closed structure is shown in darker line. The arrow shows the direction of the small-lobe movement deduced from a comparison of the open and closed conformations. The donor site (F239C) in the large lobe and acceptor site (C343) at the C-terminal tail anchored to the small lobe are highlighted in both open and closed conformation. (b) A drawing of the C subunit of cAPK with the site of cysteine substitution and FM labeling for the TRFA studies highlighted. (c) The catalytic cycle of C subunit with the rate constants from Shaffer & Adams.[28]

induce this closure. For example, small-angle X-ray scattering data show that PKI(5-22), a heat-stable protein kinase inhibitor fragment induces a contraction of the C subunit that can be explained only by domain closure,[8] but PKI(5-24) has no substantial effect on the solute accessibility (as measured by protein footprinting) to the C subunit.[9] ATP, on the other hand, produces dramatic changes in solute accessibility that are consistent with domain closure. Similarly, the analysis of ligand-induced thermostabilization, which should presumably reflect conformational ordering associated with domain closure, reveals that, in the presence of excess magnesium, ATP and ADP, but not PKI(5-24), increase the thermal stability of the C subunit.[10]

Because these conflicting results could be reconciled if there were ligand-dependent differences in the conformational dynamics of the C-subunit closed states, and because ligand-dependent conformational dynamics may play a novel role in cAPK catalysis, we developed a new method to measure cAPK domain closure and examined the state of domain closure and small-lobe flexibility at major steps of the cAPK catalytic cycle. Specifically, fluorescein 5-maleimide (FM), an energy donor, was attached to a site of cysteine substitution (F239C) in the large lobe and tetramethylrhodamine 5-maleimide (TMRM), an energy acceptor, was conjugated to the native Cys343 in the C-terminal tail, which is anchored to the small lobe (Figure 1(a)). To accomplish this, a double mutant (C199A/F239C) was engineered that permitted the selective labeling of F239C in the presence of MgATP and the native C343 in the absence of MgATP. With this approach, domain closure was monitored as an increase in the efficiency of fluorescence resonance energy transfer (FRET) as the distance between lobes shortens. Time-resolved fluorescence anisotropy (TRFA) was used to monitor the backbone flexibility of a portion of the small lobe, which was previously shown to be sensitive to the binding of ATP and PKI(5-24).[11] This was accomplished by preparation of a second mutant (K81C) that allowed the selective attachment of FM in the presence of MgATP to the tip of the small lobe at the end of the B helix (Figure 1(b)).

The FRET measurements demonstrated that both substrates/pseudosubstrates (ATP and PKI(5-24), a pseudosubstrate) and products (ADP and PO_4-PKS) induce domain closure, indicating that, with the exception of the fully dissociated state, each step of the catalysis is in a predominantly closed state. The TRFA results, however, indicate that the ligands differentially altered the conformational dynamic of the C subunit. The apparent conflicts between the previous X-ray scattering, protein footprinting, and thermostability results can be reconciled if ligands can differentially affect the closed-state dwell time. Assuming the effects of pseudosubstrates and substrates are the same, the TRFA results also reveal that only substrates/pseudosubstrates substantially reduced the backbone flexibility around the Lys81Cys site and possibly a large portion of the small lobe. This dichotomy between substrate/pseudosubstrate and product effects on small-lobe flexibility suggests the existence of an order-disorder transition coinciding with the phosphoryl transfer step that points to an internal entropy contribution to catalysis.

Results

Characterization of the mutants and their conjugates

Sequencing analysis verified the nature and location of the desired mutations for the three mutants used (K81C, C199A, and F239C/C199A). An unplanned point substitution, Asp141Glu, in the F239C/C199A mutant was discovered. Because this unplanned substitution retained the charge of the substituted amino acid and did not significantly affect the catalytic activity (data not shown), the protein was used for the FRET experiments. The SDS-PAGE analysis of the FM-labeled K81C mutant revealed no detectable, non-covalently bound probe; however, a faint fluorescent band running near the buffer front was associated with doubly labeled F239C/C199A mutant, indicating the presence of a small amount (<5 %) of non-conjugated probe (data not shown). Also, the parallel labeling of the wild-type C subunit showed no detectable labeling of the native cysteine residues (Cys199 and Cys343) by SDS-PAGE analysis, demonstrating the specificity of labeling procedures. The stoichiometry of FM labeling at F239C and TMRM presumably labeling at C343 for the F239C/C199A mutant, was ~68 % and ~57 %, respectively, which means that about 39 % of the protein was heterochromatically labeled. The stoichiometry of FM labeling of K81C and TMRM of C199A were both about 53 %. Analysis of the catalytic activity of the labeled mutants showed them to be essentially unchanged by the mutation and conjugation reactions (data not shown).

Intramolecular FRET

The control emission decay from the donor-only sample was well fit to a single-exponential expression (4.49(±0.01) ns; Table 1). In the presence of acceptor, the donor emission decay was well fit by a biexponential expression with the slower decay component (4.45(±0.03) ns; Table 1), essentially identical with the donor-only sample. The second component was 70 % faster and had an amplitude that constituted 50 % of the total decay amplitude. These results are consistent with the plus-acceptor samples being a mixture of heterochromatically labeled (donor plus acceptor) and homochromatically labeled protein.

Ligand binding reduced the lifetime of the FRET-dependent decay component. Because the ligand had little or no effect upon the donor-only

Table 1. Summary of FRET results where the donor is FM attached to F239C and the acceptor is TMRM attached to C343

Condition	τ_1 (ns)[a]	τ_2 (ns)[b]	a_2^c	χ_r^2				
A. *Donor-only*								
Apo	4.49 ± 0.01	-	-	1.2 ± 0.1				
ATP	4.49 ± 0.01	-	-	1.3 ± 0.1				
PKI(5-24)	4.56 ± 0.02	-	-	1.2 ± 0.1				
ATP + PKI(5-24)	4.59 ± 0.02	-	-	1.3 ± 0.1				
ADP + PO_4-PKS	4.58 ± 0.02	-	-	1.2 ± 0.1				
ADP	4.50 ± 0.01	-	-	1.2 ± 0.1				
					Efficiency[d]	Q_D[e]	R_0 (Å)[f]	Distance (Å)[g]
B. *Donor + acceptor*								
Apo	4.45 ± 0.03	1.32 ± 0.06	0.50 ± 0.02	1.2 ± 0.1	0.70 ± 0.01	0.27	50.0	43.2 ± 0.4
ATP	4.45 ± 0.02	1.10 ± 0.02	0.49 ± 0.01	1.3 ± 0.1	0.75 ± 0.01	0.23	48.7	40.4 ± 0.2
PKI(5-24)	4.54 ± 0.01	0.99 ± 0.05	0.44 ± 0.01	1.3 ± 0.1	0.78 ± 0.01	0.28	50.4	40.7 ± 0.4
ATP + PKI(5-24)	4.51 ± 0.01	1.06 ± 0.05	0.51 ± 0.01	1.3 ± 0.1	0.77 ± 0.01	0.27	50.0	40.9 ± 0.3
ADP + PO_4-PKS	4.51 ± 0.01	0.82 ± 0.03	0.43 ± 0.01	1.2 ± 0.1	0.82 ± 0.01	0.29	50.5	39.4 ± 0.3
ADP	4.41 ± 0.02	1.07 ± 0.05	0.47 ± 0.01	1.3 ± 0.1	0.76 ± 0.01	0.23	48.7	40.3 ± 0.3

The results (±SD) represents the mean of, at least, three measurements. The concentration of C subunit, ATP, ADP, PKI(5-24) and product (PO_4-PKS) were 200 nM, 0.5 mM, 0.5 mM, 110 μM and 110 μM, respectively. $MgCl_2$ (2.5 mM) was present in all samples containing nucleotide.

[a] The donor-only emission decay profiles were fit to a single-exponential expression.

[b] The plus acceptor emission decay profiles were fit to a biexponential decay expression.

[c] Fractional amplitude of τ_2 decay.

[d] Apparent energy transfer efficiency (equation (4)) using τ_1 as an estimate of the donor emission in the absence of acceptor (τ_D).

[e] Donor quantum yield relative to the quantum yield of fluorescein in 0.1 M NaOH at 22 °C (0.95).

[f] Förester critical distance, R_0, equals 9.765×10^3 (κ^2 J Q_D n^{-4})$^{1/6}$. κ^2 is the orientation factor that was set to 0.67, n is the refractive index (set equal to 1.4), and J is the overlap integral. J was calculated with the expression $J = \Sigma\ I_D\ (\lambda)\varepsilon_A\ (\lambda)\lambda^4\Delta\lambda / \Sigma I_D\ (\lambda)\Delta\lambda$, where $\varepsilon_A(\lambda)$ is the molar extinction coefficient of the energy acceptor and $I_D(\lambda)$ is the intensity of donor in the absence of acceptor at wavelength λ (cm). The measured value of J was 3.08×10^{-13} cm^3 M^{-1}.

[g] Calculated apparent intersite distance, R, between donor and acceptor using the expression $R = R_0\ (1/E - 1)^{1/6}$, where E equals the efficiency of energy transfer.

lifetime (Table 1), these reductions reflect the differences in the efficiency of FRET and, presumably, the distance between the donor (FM-F239C) on the large lobe and the acceptor (TMRM-C343) on the C-terminal tail, anchored to the small lobe. In the absence of any ligand, the calculated intramolecular distance was 43.2 Å (Figure 2 and Table 1). This distance compares favorably with the X-ray crystallographic distance (40.3 Å) between the α-carbon atoms of residues F239 and C343 in the C-subunit in the open conformation (using PDB code 1ctp). (We are, of course, assuming here that the open crystal structure, a binary PKI(5-24):C-subunit complex, is comparable to the open solution structure, apo form. The possibility that the intersite distance between F239 and C343

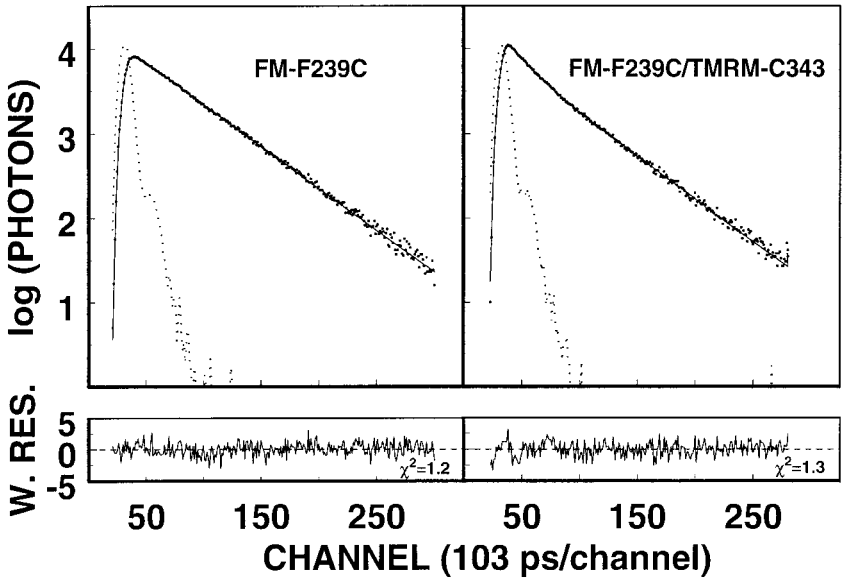

Figure 2. Fluorescence decay profiles of donor-only (FM-F239C) and donor-acceptor pair (FM-F239C/TMRM-C343). The smooth lines through experimental data were generated with best-fit parameters (Table 1) for a single-exponential (donor-only, left panel) or a double-exponential (donor-acceptor, right panel) equation. The flashlamp profile is shown as a dotted line. Weighted residuals of each corresponding curve fit are plotted in the lower panels. Experimental details are described in the Materials and Methods.

in solution differs from the crystal state cannot be ruled out.) Except for the combination of ADP and product, all the ligands studied reduced the intramolecular distance to essentially the same extent, 2.3-2.9 Å (Table 1). The magnitude of this reduction in intramolecular distance corresponds well to the difference in distance (1.8 Å) between α-carbon atoms of residues F239 and C343 in the open and closed conformations (comparing PDB codes 1ctp, open, with 1atp, closed). Consequently, the FRET results suggest that the observed ligand-induced shorting of the distance between FM-F329C and TMRM-C343 correlates with the hinge and sliding motions of the small lobe relative to the large lobe that defines the closure of the active-site cleft.

ADP plus PO_4-PKS reduced the apparent donor-acceptor (D/A) intersite distance by about 3.8 Å, significantly more than the other ligands. Because of the steric limits to how far the small and large lobes can move toward each other, this greater reduction in intramolecular FRET probably represents either a specific ligand-dependent shift in the position/orientation of reporter groups or a movement of just the C-terminal tail toward the large lobe. Whichever is true, the results suggest strongly that the combination of ADP plus product, like the other ligands studied, induced a closed conformation of the C subunit.

To confirm the binding-dependent character of these changes, FRET between FM-F239C and TMRM-C343 was measured in the presence of nucleotides and increasing concentrations of PKI(5-24) and PO_4-PKS. PKI(5-24), which binds with low affinity to the C subunit in the absence of ATP, was associated with concentration-dependent reduction in the D/A distance until the effect plateaued between 23 μM and 100 μM, suggesting that PKI(5-24) is fully bound at a concentration of 100 μM in the absence of ATP (Figure 3). In the presence of ATP, which markedly increases the affinity of PKI(5-24) toward the C subunit, PKI(5-24) titration produced no further significant change in the D/A pair distance, indicating that ATP alone closes the active-site cleft. As with ATP, ADP alone reduced the D/A pair intersite distance, and the addition of product (PO_4-PKS) was associated with a further increase in FRET that plateaued between 38.8 and 39.2 Å. Both in the presence and the absence of ATP, the effects of PKI(5-24) plateaued at the same intermolecular distance, 40.6 and 40.9 Å.

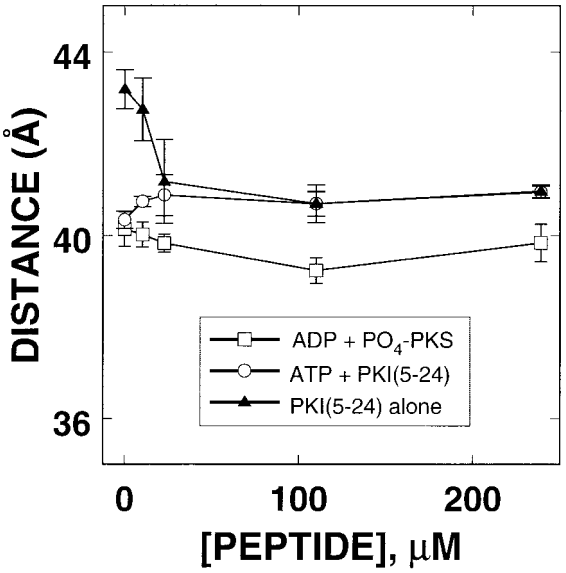

Figure 3. Concentration-dependence of peptide-induced changes in the distance between FM-F239C and TMRM-C343. The concentration-dependence of peptidyl substrates (PKI(5-24) only, filled triangles; PKI(5-24) plus ATP, open circles) and products (PO_4-PKS plus ADP, open squares) induced changes in the apparent intersite distance (mean ± SD) between FM-239C and TMRM-C343 at 22 °C. The concentrations of FM-F239C/TMRM-C343, ATP, ADP were 0.2 μM, 0.5 mM, and 0.5 mM, respectively. $MgCl_2$ (2.5 mM) was present in all samples containing nucleotide.

FM-K81C anisotropy decay

To assess possible linkages between large-scale domain movements, local segmental flexibility, and the catalytic process, the effect of ligand binding upon the TRFA of FM attached to K81C was examined. The K81C site was chosen because it is located in the conformationally active small lobe, and because it was observed previously that ATP plus PKI(5-24) dramatically reduces the backbone flexibility around this mutation/conjugation site.[11] Control experiments indicated that the ligands studied had no significant effect upon either the wavelength maximum or the fwhm (full width at half-maximum) of the FM-K81C conjugate; the values ranged between 516-518 nm and 28-29 nm, respectively. Additionally, the emission decay profile was well fit to a biexponential decay function (Figure 4). Ligand binding, again, had little or no effect upon the emission decay kinetics; the values of the slow and fast emission lifetimes ranged between 4.20-4.26 ns (81-84 % of total amplitude) and 2.48-2.54 ns, respectively (data not shown). For brevity, only the geometric averaged lifetimes are presented in Table 2 and ranged between 3.88 and 3.99 ns.

The TRFA decay of apo FM-K81C (Figure 4) was well fit by a model-free, non-associative biexponential function (equation (7)). The ''fast'' rotational correlation time, ϕ_{fast}, and the fractional amplitude of the ''fast'' decay processes, f_{xb}, which largely reflect backbone flexibility around the site of conjugation, were 1.9 ns and 0.31, respectively (Table 2). Assuming a wobbling-in-a-cone diffusion model,[12] the f_{xb} term should be determined by the cone angle, therefore, represent the amplitude of the diffusion motion, and the ratio ϕ_{fast}/f_{xb} should be a function of the diffusion rate. The value of the ''slow'' correlation time ranged between 20 ns and

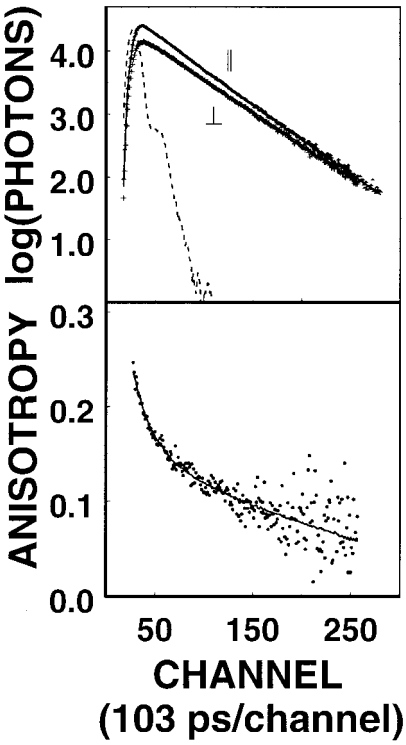

Figure 4. Emission and anisotropy decay of FM-K81C. The upper panel illustrates the parallel (‖) and perpendicular (⊥) emission decays (single datum points), a smooth line through these points was generated with the best-fit parameters for a biexponential decay equation. The flashlamp profile is shown as a dotted line. The lower panel shows the time-resolved anisotropy decay (single datum points) and a smooth line through these points generated with the best-fit parameters (Table 2) for a biexponential, non-associative model (equation (7)). Measurements were taken at 22 °C, and the concentration of FM-K81C was 0.2 μM.

25 ns, which is expected (21.3 ns) from the Stokes-Einstein equation for a molecule with the hydrodynamic radius of the C subunit (27.4 Å).[13] Thus, the ϕ_{slow} largely reflects whole-body rotational diffusion and does not include any detectable intermediate speed (between ϕ_{fast} and ϕ_{slow}) internal motions that would accelerate the observed ''slow'' anisotropy decay component.

All the ligands studied reduced the amplitude of the fast anisotropy decay to some degree and perturbed the ϕ_{fast} values in complex ways without substantially affecting either the slow anisotropy decay or the time-zero anisotropy (Table 2). The effects upon ϕ_{fast} and f_{xb} were complex and difficult to categorize by themselves, but visual comparison of the convolved-anisotropy decay profiles (Figure 5) and examination of the best-fit ϕ_{fast}/f_{xb} ratios (Table 2) shows that the ligands can be grouped into three categories based on the magnitude of their effects. ATP plus PKI(5-24) induced the most dramatic reduction in the amplitude and rate of anisotropy decay (Figure 5(a); with ϕ_{fast}/f_{xb} decreasing from 0.17 to 0.09) suggesting the backbone flexibility around K81C was reduced the most by this ligand combination. Alone, ATP and PKI(5-24) each produced the same effect (Figure 5(d) and (f)), which was to reduce the mobility of the reporter group to about half the extent as the combination of these two ligands (ϕ_{fast}/f_{xb} ratio shifted from 0.17 to 0.12-0.13). Finally, ADP alone or in combination with product produced the same effect (Figure 5(b) and (e)), which was to marginally slow the anisotropy decay of FM-K81C without significantly changing the ϕ_{fast}/f_{xb} ratio (the ϕ_{fast}/f_{xb} ratio shifted from 0.17 to 0.15-0.16; Table 2). Thus, only the substrate/pseudosubstrates, alone or together, substantially altered the segmental flexibility around K81C at the tip of the small lobe.

Technical note

Although we confirmed our previous observation that the combination of PKI(5-24) and ATP greatly decreases the amplitude and rate of FM-K81C anisotropy decay,[11] the values of the anisotropy decay parameters presented here (Table 2) differ from the earlier report. This difference probably reflects improvements in both the instrumental setup (more stable flashlamp and detector) and data analysis protocol (emission-lifetime parameters determined independently of the anisotropy parameters). In spite of the technical shortcomings of the previous study, we believe in the validity of its basic conclusion, that the fast anisotropy-decay components reflect backbone fluctuations around surface sites of cysteine substitution and FM conjugation.

Discussion

Adjacent structural elements within proteins interact to create a responsive network that can extend throughout the entire protein and can be differentially perturbed by the binding of small molecules and heteroproteins. In the case of the cAPK C subunit, each ligand examined produced a unique response pattern that changed both the conformation and dynamics of the protein. Although all the ligands examined induced domain closure, the combination of ADP plus product induced a specific conformational change (local or large scale) that further enhanced the D/A energy transfer between the large and small lobes. In terms of the flexibility around the B helix, the effects of PKI(5-24) and ATP alone reduced segmental flexibility to about the same extent, and these effects were additive in the ternary complex (ATP:PKI(5-24):C). In contrast, ADP alone or in combination with the product had a minimal effect on the flexibility around the B helix.

The basis for the greater thermal stability[10] and reduced solute accessibility[9] of the binary ATP:C subunit compared with the PKI(5-24):C subunit complex, which was the impetus for this project,

Table 2. Effect of substrates and products on the anisotropy decay parameters of FM-K81C

Condition	r_o [a]	f_{xb} [b]	ϕ_{fast} [c] (ns)	ϕ_{slow} [d] (ns)	f_{xb}/ϕ_{fast} [e]	χ_r^2	$\langle\tau\rangle$ [f] (ns)
Apo	0.25 ± 0.00	0.31 ± 0.02	1.9 ± 0.1	20-25	0.17 ± 0.02	1.3 ± 0.1	3.99 ± 0.01
ATP	0.25 ± 0.01	0.20 ± 0.04	1.7 ± 0.2	20-24	0.12 ± 0.01	1.1 ± 0.1	3.93 ± 0.01
PKI(5-24)	0.25 ± 0.00	0.22 ± 0.02	1.7 ± 0.3	21-25	0.13 ± 0.01	1.4 ± 0.1	3.91 ± 0.01
ATP + PKI(5-24)	0.27 ± 0.01	0.20 ± 0.02	2.3 ± 0.4	19-23	0.09 ± 0.01	1.1 ± 0.1	3.88 ± 0.01
ADP + PO_4-PKS	0.25 ± 0.01	0.23 ± 0.01	1.5 ± 0.2	20-25	0.15 ± 0.02	1.3 ± 0.1	3.89 ± 0.01
ADP	0.25 ± 0.00	0.23 ± 0.04	1.5 ± 0.2	20-25	0.16 ± 0.01	1.3 ± 0.1	3.95 ± 0.01

The results (±SD) represent the mean of, at least, three determinations. The vertically and orthogonally polarized emission decays were analyzed simultaneously for the parameters of $S(t)$ (equation (6)) and $r(t)$ (equation (7)) with the Globals Unlimited™ computer program. The experimental details are described under Materials and Methods. The concentration of C subunit, ATP, ADP, PKI(5-24) and product (PO_4-PKS) were 0.2 μM, 0.5 mM, 0.5 mM, 239 μM and 239 μM, respectively. $MgCl_2$ (2.5 mM) was present in all samples containing nucleotide.

[a] The time-zero anisotropy.
[b] The fraction of the observed anisotropy decay associated with the fast depolarization processes.
[c] Fast rotational correlation time.
[d] The range of the slow rotational correlation times that yielded χ_r^2 values 5% above the minimum.
[e] Value that is function of the diffusion rate constant.
[f] Geometric averaged lifetimes ($\Sigma\alpha_i\tau_i$, where $\Sigma_i = 1$).

probably rests with differences in the closed-state dwell times between the binary PKI(5-24):C and ATP:C subunit complexes. The PKI(5-24):C subunit complex, unlike the ATP complex, intermittently opens, allowing transient solute accessibility but not increased thermostability. The ATP:C subunit complex, on the other hand, probably exists in a persistently closed state that both reduces solute accessibility and increases C subunit thermostability.

The idea that the binary PKI(5-24):C subunit complex fluctuates between open and closed states is consistent with the observation that both open and closed crystals of the binary complex have been reported.[2,5] This view is further strengthened by an analysis of ATP and PKI(5-24)-mediated bilobular connections. The adenosine ring of ATP is packed tightly into the base of the cleft between the two lobes with N6 hydrogen bonding directly to the backbone Glu121 in the bilobular linker

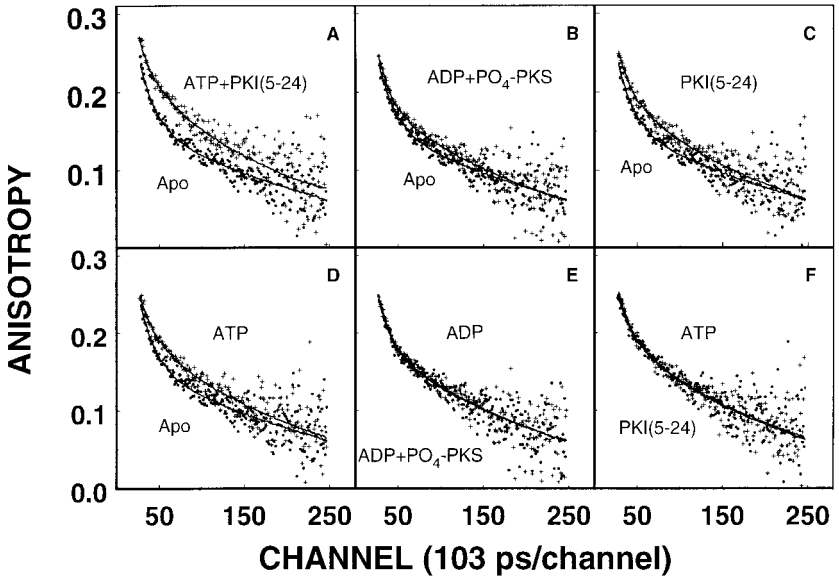

Figure 5. Effect of substrates and products on the anisotropy decay profiles of FM-K81C. (a) FM-K81C in the absence (filled circles) and the presence of ATP plus PKI(5-24) (pseudosubstrate, plus symbols). (b) FM-K81C in the absence (filled circles) and the presence of ADP plus product (PO_4-PKS, plus symbols). (c) FM-K81C in the absence (filled circles) and the presence of PKI(5-24) (pseudosubstrate, plus symbols). (d) FM-K81C in the absence (filled circles) and the presence of ATP (substrate, plus symbols). (e) FM-K81C in the presence of ADP (product, filled circles) and ADP plus peptidyl product (PO_4-PKS, plus symbols). (f) FM-K81C in the presence of ATP (substrate, filled circles) and PKI(5-24) alone (pseudosubstrate, plus symbols). The concentrations of FM-K81C, PKI(5-24), PO_4-PKS, ATP and ADP were 0.2 μM, 239 μM, 239 μM, 0.5 mM, and 0.5 mM, respectively. Measurements were taken at 22 °C, and $MgCl_2$ (2.5 mM) was present in all samples containing nucleotide.

region. Also, Glu127 at the end of the linker hydrogen bonds to the 3′OH of the ribose ring. Additionally, the β-phosphate group of ATP bonds with Phe54(N), Gly55(N), and Lys72 in the small lobe. The γ-phosphate group bonds with Ser53(N) in the small lobe, Lys168 and Asn171 (mediated by Mn^{2+}) in the large lobe (PDB code 1atp). Thus, ATP mediates a large number of bilobular connections. PKI(5-24), on the other hand, mediates far fewer bilobular connections. It binds primarily to the base of the active-site crevice on the surface of the large lobe with one of its residues (Arg18 at the P-3 position) spanning the crevice to interact with both Thr51(O) and Tyr330 in the small lobe (PDB code 1apm). The minimal number of PKI(5-24)-mediated bilobular links compared with ATP probably explains why the PKI(5-24):C subunit complexes are intermittently open.

While it is probably impossible to fully delineate the response network that propagates the unique signature of each interacting ligand through the C subunit, some elements of this network can be deduced from the X-ray crystal structures of the closed ternary (ATP:PKI(5-24):C subunit; PBD code 1atp) and binary (PKI(5-24):C subunit; PDB code 1apm) complexes. For example, the γ-phosphate group of ATP, as discussed above, interacts with the amide nitrogen atom of Ser53, and the Ser53 carbonyl group is within hydrogen bonding distance of the Lys78 ε-amino group, three residues away from the site of cysteine substitution and the TRFA reporter group attachment (Lys81) in the B helix. It is not surprising, therefore, that ATP binding reduces segmental flexibility around K81C, while ADP has little or no effect. The ability of PKI(5-24) alone to reduce the segmental flexibility around the tip of the small lobe is, on the other hand, difficult to deduce. The guandino moiety of the PKI(5-24) Arg18 interacts with Thr51(O) and Tyr330; however, Lys78, in the B helix, is too far away from Ser53, in the glycine-rich loop, to form a bond that would stabilize the B helix. Similarly, although PKI(5-24) Arg18 interacts with Tyr330 in the C-terminal tail, which interacts with the surface of the small lobe, there is no direct linkage between the C-terminal tail and the B helix. Consequently, there must be an elusive linkage between PKI(5-24) binding and the B helix that might be mediated, at least in part, by Tyr330 in the C-terminal tail.

An intriguing aspect of the various ligand-induced dynamic states is that there appears to be a relation between the segmental flexibility around the B helix and whether the interacting ligand is a substrate/pseudosubstrate or a product. Assuming a correspondence of peptidyl substrate and pseudosubstrate effects, substrates, especially the combination of ATP and PKI(5-24), greatly order, at least, a portion of the small lobe and are present in the reaction pathway before the phosphoryl transfer step. Products, which minimally affect small-lobe flexibility, are present in the reaction pathway after the phosphoryl transfer step. This order-disorder dichotomy appears to be associated with the phosphoryl transfer process and suggests that there may be a positive internal entropy contribution to catalysis. Historically, the analysis of the thermodynamics of enzyme catalysis has focused on the reacting groups and the loss of entropy associated with the need to immobilize and to precisely position the reactants with respect to the catalytic moieties.[14,15] The present results appear to add another dimension to the thermodynamics of catalysis, because they suggest a role for the conformational activity of the enzyme over and above providing a platform for catalysis. Clearly, the importance of this positive entropy component in the overall thermodynamics of cAPK catalytic activity is uncertain and requires further study. Part of such a further study will be to establish the extent of the order-disorder dichotomy in the conformationally active small lobe as well as to explore ways to separate protein from water dynamics.

In summary, this study was initiated out of the possibility that the conflicting small-angle X-ray scattering, protein footprinting, and thermostability results could be reconciled, if there are ligand-dependent differences in the dynamics of C subunit closed states. An independent method (FRET) to assess domain closure in solution was developed and the segmental flexibility of a portion of the small lobe was measured by TRFA at key steps of the cAPK catalytic cycle. Combined with previous thermostability and solute accessibility results, the present work reveals that each step of the catalytic cycle examined was associated with a unique dynamic state of the C subunit, and that the hinge and sliding motion of the small lobe associated with domain closure is independent of the fluctuations of the B helix. An intriguing feature of these ligand-dependent conformational states is that the segmental flexibility around the B helix appears to depend upon whether the ligand was a substrate/pseudosubstrate or product. The substrates/pseudosubstrate reduced flexibility and products were essentially without effect. This dichotomy between substrate and product effects suggests the existence of an order-disorder transition coinciding with the phosphoryl transfer step that points to an internal entropy contribution to catalysis. Finally, the apparent conflicts between the previous X-ray scattering, protein footprinting, and thermostability results can be reconciled if ligands differentially affect the closed-state dwell time.

Materials and Methods

Materials

Fluorescein 5-maleimide and tetramethylrhodamine 5-maleimide were purchased from Molecular Probes (Eugene, OR). ATP, ADP, cAMP, and PKI(5-24) were obtained form Sigma (St. Louis, MO). Non-phosphorylated-PKS (TTYADFIASGRTGRRASIHD) was a gift from Dr E. A. Komives at the University of California, San

Diego. This peptide was phosphorylated at Ser21 with cAPK and purified by HPLC. The mutant C subunits (F239C/C199A, C199A, and K81C) were prepared and characterized as described.[16–18]

Fluorescein (FM) and tetramethylrhodamine (TMRM) maleimide labeling of F239C/C199A

The mutant C subunit (1-2 mg) was initially buffer-exchanged by elution through a Sephadex G-25 column (2.5 cm × 7 cm) equilibrated with buffer A (20 mM Mops (pH 7.5), 100 mM KCl). The protein fractions were pooled and the concentration of the pooled samples was determined with UV/visible spectrometry using an ε_{280} of 45,000 M^{-1} cm^{-1}. To protect the C343 site from labeling, ATP (4 mM) and $MgCl_2$ (6 mM) were added to the reaction mixture prior to the addition of a twofold molar excess of FM to protect the Cys343 from being labeled.[19] A parallel control sample in which wild-type C subunit was treated like the mutant protein was used to assess the specificity of labeling. The protein concentration of the reaction mixture ranged between 6 and 8 μM. The reactions were allowed to proceed for one hour at room temperature, protected from light, and then eluted through a Sephadex G-25 column (2.5 cm × 7 cm) equilibrated with buffer B (20 mM Mops (pH 7.5), 1 M KCl) at room temperature. The FM-labeled protein fractions were then pooled and concentrated to a final concentration of about 5 μM. A portion of the FM-labeled sample was set aside for donor-only measurements. To heterochromatically label the mutant, a 1.5-fold molar excess of TMRM was added to the FM-labeled protein and the reaction was allowed to proceed for one hour at room temperature, protected from light. Unconjugated TMRM was then removed by Sephadex G-25 chromatography and aggregated protein was separated from monomeric by Sephacryl S-200 chromatography. Fluorescein emission (excitation at 470 nm and emission at 525 nm) from the column fractions was measured, and the fluorescent fractions with retention times that corresponded to unmodified C subunit were pooled. Aliquots of the pooled fractions were subjected to gel electrophoresis under denaturing conditions (SDS-12 % PAGE)[20] and the fluorescent bands were visualized with a mineral lamp to assess the presence of any unconjugated FM or TMRM in the sample, which migrates near the buffer front.

Labeling of K81C and C199A

The preparation of FM-K81C was exactly the same as that of the FM-F239C/C199A, except that the K81C mutant was initially buffer-exchanged by elution through a Sephadex G-25 column (1.5 cm × 7 cm) equilibrated with buffer D (20 mM Mops (pH 7.1), 100 mM KCl). The TMRM labeling of Cys343 on the C199A mutant was prepared like FM-K81C, except MgATP was not added to the reaction mixture. As with labeling the F239C/C199A mutant, a parallel wild-type C subunit was prepared to assess the specificity of labeling.

Phosphotransferase assay

The activity of the labeled C mutants was quantified by the method of Cook *et al.*[21] with kemptide as a substrate.

Determination of the stoichiometry of labeling

The stoichiometry of FM-labeled C subunits was estimated spectrophotometrically by substitution of the measured absorbance values at 280 nm (A_{280}) and 497 nm (A_{497}) into the expression:

$$\frac{[\text{Fluorescein}]}{[\text{C subunit}]} = \frac{A_{497}/83{,}000}{(A_{280} - 0.18A_{497})/45{,}000} \quad (1)$$

The stoichiometry of TMRM-labeled C subunits was estimated spectrophotometrically by substitution of the measured absorbance values at 280 nm (A_{280}), 497 nm (A_{497}) and 554 nm (A_{554}) into the expression:

$$\frac{[\text{TMRM}]}{[\text{C subunit}]} = \frac{A_{554}/91{,}000}{(A_{280} - 0.18A_{497} - 0.18A_{554})/45{,}000} \quad (2)$$

The stoichiometry of heterochromatically labeled C subunit was determined using the following equation:

$$C_{\text{FM-TMRM}}\% = \frac{[\text{Fluorescein}]}{[\text{C subunit}]} \times \frac{[\text{TMRM}]}{[\text{C subunit}]} \quad (3)$$

Steady-state emission spectra

Steady-state emission spectra were measured at room temperature using an Instrument S.A., Inc. Jobin Yvon/Spex FluoroMax II spectrofluorometer.

Fluorescence lifetime

Fluorescence lifetimes were determined by the time-corrected single-photon counting technique.[22] Excitation and emission bands were selected with Omega 470-DF-D35 and Oriel 520-nm narrow-band interference filters, respectively. In addition to the chromatic filters, Polaroid HNP'B dichroic film polarizers (Norwood, MA) were placed in the path of the excitation and emission beams. The excitation polarizer was oriented vertically and the emission polarizer was rotated at an angle of 54° from vertical to minimize anisotropic contributions to the observed decay.

The efficiency (E) of dipolar resonance energy transfer between the donors and acceptors was measured as the extent of the reduction of the donor fluorescence lifetime:

$$E = 1 - \tau_{DA}/\tau_D \quad (4)$$

τ_{DA} and τ_D are the fluorescence lifetimes of the donor in the presence and absence of acceptor, respectively.[23,24]

To minimize the uncertainties associated with the intersite distance measurements, the basic FRET parameters were determined for each ligand-bound configuration examined. Using the ratio method of Chen,[25] the quantum yield, Q_D, of the apo form of FM-F239C/C199A was determined to be 0.27 relative to the Q_D of fluorescein (0.95) in 0.1 M NaOH at 22 °C.[26] The Q_D values for the ligand-bound configurations were estimated from the effect of the ligands on the integrated area beneath the corrected emission spectra of FM-F239C/C199A.

Because of low yields, the normalized excitation spectrum of the TMRM-C199A mutant was used to estimate the acceptor absorption spectrum. Setting the value of the absorption maximum, ε_{max}, of TMRM to 91,000 M^{-1} cm^{-1} (the value of the β-mercaptoethanol adduct in

methanol), the molar extinction spectrum, $\varepsilon(\lambda)$, was generated and, with the donor emission spectrum of FM-F239C/C199A, the overlap integral, J, was calculated to be 3.08×10^{-13} cm^3 M^{-1} (Table 1). This same value of J was used for all the FRET conditions, because the ligands studied had no significant effect upon the excitation or emission λ_{max} values of FM-F239C/C199A or TMRM-C343 in the C199A mutant. Making the usual assumptions that κ^2 equals 2/3, and the FRET efficiency was quantified by the analysis of the FM-donor lifetime.

Time-resolved fluorescence anisotropy

The emission anisotropy was determined by time-correlated single-photon counting measurements as described.[27] Briefly, the vertically ($I_{\parallel}(t)$) and orthogonally ($I_{\perp}(t)$) polarized emission components were collected by exciting samples with vertically polarized light while orienting the emission polarizer (Polaroid HNPNB dichroic film) in either a vertical or orthogonal direction. Excitation and emission bands were selected with an Oriel 500-nm short-pass interference (catalog no. 59876) and a Corning 3-68 cuton filter, respectively. The polarization bias (G) of the detection instrumentation was determined by measuring the integrated photon counts/6×10^6 lamp flashes while the samples were excited with orthogonally polarized light and the emission was monitored with a polarizer oriented in the vertical and orthogonal directions ($G = 1.028$).

The emission anisotropy decay, $r(t)$, given by the expression:

$$r(t) = \frac{(I_{\parallel}(t) - GI_{\perp}(t))}{(I_{\parallel}(t) + 2G \cdot I_{\perp}(t))} \tag{5}$$

and total emission decay, $S(t)$, for a macroscopically-isotropic sample:

$$S(t) = I_{\parallel}(t) + 2G \cdot I_{\perp}(t) \tag{6}$$

were deconvolved simultaneously from the individual polarized emission components.

With the Globals Unlimited™ computer program, the $I_{\parallel}(t)$ and $I_{\perp}(t)$ decay profiles were deconvolved simultaneously for the parameters of $S(t)$ and $r(t)$. Here, $r(t)$ is the anisotropy decay function:

$$\begin{aligned} r(t) = {} & r_o f_{xb} \exp(-t/\phi_{fast}) \\ & + r_o(1 - f_{xb}) \exp(-t/\phi_{slow}) \end{aligned} \tag{7}$$

where r_o is the amplitude of the anisotropy at time zero, f_{xb} is the fraction of the anisotropy decay associated with the fast decay processes, and ϕ is the rotational correlation time of the anisotropy decay. The subscripts fast and slow denote the fast and slow decay processes, respectively. A non-associative model was assumed, indicating that the rotational correlation times are common to each of the emission relaxation times. Goodness of fit was evaluated from the value of the reduced χ_r^2 and visual inspection of the weighted-residual plot.

The uncertainty of the measured slow rotational correlation times, ϕ_{slow}, was quantified as a range. This involved directed unidimensional searches along the ϕ_{slow} parameter axis, which did not allow other fitting parameters to vary, to find the minimum and maximum ϕ_{slow} values that raised the χ_r^2 values by 5%.

Acknowledgments

We thank Siv Garrod for phosphorylating and purifying PKS. This work was supported by a grant from the National Institutes of Health (GM 19301) to S.S.T.

References

1. Anderson, C. M., Zucker, F. H. & Steitz, T. A. (1979). Space-filling models of kinase clefts and conformation changes. *Science,* **204**, 375-380.
2. Zheng, J., Knighton, D. R., Xuong, N. H., Taylor, S. S., Sowadski, J. M. & Ten, Eyck L. F. (1993). Crystal structures of the myristylated catalytic subunit of cAMP-dependent protein kinase reveal open and closed conformations. *Protein Sci.* **2**, 1559-1573.
3. Zheng, J. H., Trafny, E. A., Knighton, D. R., Xuong, N. H., Taylor, S. S., Teneyck, L. F. & Sowadski, J. M. (1993). 2.2 Å refined crystal-structure of the catalytic subunit of cAMP-dependent protein-kinase complexed with MnATP and a peptide inhibitor. *Acta Crystallog. sect. D,* **49**, 362-365.
4. Bossemeyer, D., Engh, R. A., Kinzel, V., Ponstingl, H. & Huber, R. (1993). Phosphotransferase and substrate binding mechanism of the cAMP-dependent protein kinase catalytic subunit from porcine heart as deduced from the 2.0 Å structure of the complex with Mn^{2+} adenylyl imidodiphosphate and inhibitor peptide PKI(5-24). *EMBO J.* **12**, 849-859.
5. Knighton, D. R., Bell, S. M., Zheng, J. H., Ten Eyck, L. F., Xuong, N. H., Taylor, S. S. & Sowadski, J. M. (1993). 2.0 Å refined crystal-structure of the catalytic subunit of cAMP-dependent protein-kinase complexed with a peptide inhibitor and detergent. *Acta Crystallog. sect. D,* **49**, 357-361.
6. Madhusudan, Trafny, E. A., Xuong, N. H., Adams, J. A., Ten Eyck, L. F., Taylor, S. S. & Sowadski, J. M. (1994). cAMP-dependent protein kinase: crystallographic insights into substrate recognition and phosphotransfer. *Protein Sci.* **3**, 176-118.
7. Narayana, N., Cox, S., Nguyen-huu, X., Ten Eyck, L. F. & Taylor, S. S. (1997). A binary complex of the catalytic subunit of cAMP-dependent protein kinase and adenosine further defines conformational flexibility. *Structure,* **5**, 921-935.
8. Olah, G. A., Mitchell, R. D., Sosnick, T. R., Walsh, D. A. & Trewhella, J. (1993). Solution structure of the cAMP-dependent protein kinase catalytic subunit and its contraction upon binding the protein kinase inhibitor peptide. *Biochemistry,* **32**, 3649-3657.
9. Cheng, X., Shaltiel, S. & Taylor, S. S. (1998). Mapping substrate-induced conformational changes in cAMP-dependent protein kinase by protein footprinting. *Biochemistry,* **37**, 14005-14013.
10. Herberg, F. W., Doyle, M. L., Cox, S. & Taylor, S. S. (1999). Dissection of the nucleotide and metal-phosphate binding sites in cAMP-dependent protein kinase. *Biochemistry,* **38**, 6352-6360.
11. Gangal, M., Cox, S., Lew, J., Clifford, T., Garrod, S. M., Aschbaher, M., Taylor, S. S. & Johnson, D. A. (1998). Backbone flexibility of five sites on the catalytic subunit of cAMP-dependent protein kinase in the open and closed conformations. *Biochemistry,* **37**, 13728-13735.

12. Kinosita, K., Jr, Kawato, S. & Ikegami, A. (1977). A theory of fluorescence polarization decay in membranes. *Biophys. J.* **20**, 289-305.
13. Herberg, F. W., Dostmann, W. R., Zorn, M., Davis, S. J. & Taylor, S. S. (1994). Crosstalk between domains in the regulatory subunit of cAMP-dependent protein kinase: influence of amino terminus on cAMP binding and holoenzyme formation. *Biochemistry,* **33**, 7485-7494.
14. Page, M. L. & Jencks, W. P. (1971). Entropic contribution to rate accelerations in enzymic and intramolecular reactions and the chelate effect. *Proc. Natl Acad. Sci. USA,* **68**, 1678-1683.
15. Blow, D. (2000). So do we understand how enzymes work? *Structure,* **8**, R77-R81.
16. Slice, L. W. & Taylor, S. S. (1989). Expression of the catalytic subunit of cAMP-dependent protein kinase in *Escherichia coli*. *J. Biol. Chem.* **264**, 20940-20946.
17. Kunkel, T. A. (1985). Rapid and efficient site-specific mutagenesis without phenotypic selection. *Proc. Natl Acad. Sci. USA,* **82**, 488-492.
18. Lew, J., Coruh, N., Tsigelny, I., Garrod, S. & Taylor, S. S. (1997). Synergistic binding of nucleotides and inhibitors to cAMP-dependent protein kinase examined by acrylodan fluorescence spectroscopy. *J. Biol. Chem.* **272**, 1507-1513.
19. First, E. A. & Taylor, S. S. (1989). Selective modification of the catalytic subunit of cAMP-dependent protein kinase with sulfhydryl-specific fluorescent probes. *Biochemistry,* **28**, 3598-3605.
20. Laemmli, U. K. (1970). Cleavage of structural proteins during the assembly of the head of bacteriophage T4. *Nature,* **227**, 680-685.
21. Cook, P. F., Neville, M. E., Jr, Vrana, K. E., Hartl, F. T. & Roskoski, R., Jr (1982). Adenosine cyclic 3′,5′-monophosphate dependent protein kinase: kinetic mechanism for the bovine skeletal muscle catalytic subunit. *Biochemistry,* **21**, 5794-5799.
22. Yguerabide, J. (1972). Nanosecond fluorescence spectroscopy of macromolecules. *Methods Enzymol.* **26**, 498-578.
23. Foster, T. (1959). 10th Spier memorial lecture. Transfer mechanisms of electronic exciation. *Discuss. Faraday Soc.* **27**, 7-17.
24. Stryer, L., Thomas, D. D. & Carlsen, W. F. (1982). Fluorescence energy transfer measurements of distances in rhodopsin and the purple membrane protein. *Methods Enzymol.* **81**, 668-678.
25. Chen, R. F. (1967). Fluorescence quantum yields of tryptophan and tyrosine. *Anal. Letters,* **1**, 35-42.
26. Brannon, J. H. & Magde, D. (1978). Absolute quantum yield determination by thermal blooming. Fluorescein. *J. Phys. Chem.* **82**, 705-709.
27. Li, F., Gangal, M., Jones, J. M., Deich, J., Lovett, K. E., Taylor, S. S. & Johnson, D. A. (2000). Consequences of cAMP and catalytic-subunit binding on the flexibility of the A-kinase regulatory subunit. *Biochemistry,* **39**, 15626-15632.
28. Shaffer, J. & Adams, J. A. (1999). Detection of conformational changes along the kinetic pathway of protein kinase A using a catalytic trapping technique. *Biochemistry,* **38**, 12072-12079.

Edited by A. Fersht

(Received 21 June 2001; received in revised form 9 November 2001; accepted 15 November 2001)